Bone 112 (2018) 42–50

Contents lists available at ScienceDirect

Bone

journal homepage: www.elsevier.com/locate/bone

Full Length Article

Epiphyseal growth plate architecture is unaffected by early postnatal activation of the expression of R992C collagen II mutant

Jolanta Fertala[a,1], Machiko Arita[a,1], Andrzej Steplewski[a], William V. Arnold[a,b], Andrzej Fertala[a,*]

[a] Department of Orthopaedic Surgery, Sidney Kimmel Medical College, Thomas Jefferson University, Philadelphia, PA, USA
[b] Rothman Institute of Orthopaedics, Thomas Jefferson University Hospital, Philadelphia, PA, USA

ARTICLE INFO

Keywords:
Collagen mutations
Collagen II
Cartilage
Spondyloepiphyseal dysplasia
Growth plate

ABSTRACT

Spondyloepiphyseal dysplasia (SED) exemplifies a group of heritable diseases caused by mutations in collagenous proteins of the skeletal system. Its main feature is altered skeletal growth. Pathomechanisms of SED include: changes in the stability of collagen II molecules, inability to form proper collagen fibrils, excessive intracellular retention of mutant molecules, and endoplasmic reticulum stress. The complexity of this pathomechanism presents a challenge for designing therapies for SED. Our earlier research tested whether such therapies only succeed when applied during a limited window of development. Here, employing an inducible mouse model of SED caused by the R992C mutation in collagen II, we corroborate our earlier observations that a therapy must be applied at the prenatal or early postnatal stages of skeletal growth in order to be successful. Moreover, we demonstrate that blocking the expression of the R992C collagen II mutant at the early prenatal stages leads to long-term positive effects. Although, we could not precisely mark the start of the expression of the mutant, these effects are not significantly changed by switching on the mutant production at the early postnatal stages. By demonstrating the need for early therapeutic interventions, our study provides, for the first time, empirically-based directions for designing effective therapies for SED and, quite likely, for other skeletal dysplasias caused by mutations in key macromolecules of the skeletal system.

1. Introduction

Skeletal aberrations in patients harboring mutations in *COL2A1* emphasize the fundamental role of collagen II in the development of the skeleton [1]. Collagen II mutations cause diverse chondrodysplasia phenotypes classified as spondyloepiphyseal dysplasia (SED; OMIM 183900) [1–3]. The SED phenotypes range in severity from achondrogenesis type II, which is lethal at or before birth, to late-onset SED with early-onset osteoarthritis [1–3].

When mutant collagen II molecules are present during skeletal development, cartilage and bone are affected at the molecular, cellular, and tissue levels [1,3]. In brief, mutations in collagen II can lower the thermostability of mutant molecules, change their shape, and alter the formation of collagen II fibrils. Cartilaginous matrix that harbors collagen II mutants has aberrant architecture that may reduce the ability of growth plate chondrocytes to maintain their proper columnar arrangements, thereby limiting the growth of endochondral bones [4]. In addition, mutations that prevent proper folding of collagen chains into triple helices may increase intracellular accumulation of aberrant collagen II molecules and cause endoplasmic reticulum (ER) stress [1,5–7].

Despite significant progress in understanding the pathomechanisms of heritable skeletal dysplasias, no therapies effectively target the molecular basis of these diseases. Experimental approaches to reduce the consequences of collagen mutations have included cell therapies, gene therapies, and therapies to reduce the effects of ER stress [1,8,9]. The efficacies of growth hormone and statins to improve the growth of bones harboring mutant molecules have been also tested [10,11]. Thus far, these approaches have not been effective in preventing skeletal dysplasias.

Researchers have also tested the clinical utility of cells transplanted from healthy donors to patients with severe forms of osteogenesis imperfecta (OI), a bone dysplasia caused predominantly by mutations in collagen I. Infusions of therapeutic cells at the prenatal and the postnatal stages of skeletal growth have resulted in only minimal, transient effects [12–17]. It remains unclear whether these limited outcomes were due to the poor engraftment of donors' cells into bones or due to the ill-defined timing of cell transplantations [1,15]. To advance the

* Corresponding author at: Department of Orthopaedic Surgery, Sidney Kimmel Medical College, Thomas Jefferson University, Curtis Building, Room 501, 1015 Walnut Street, Philadelphia, PA 19107, USA.
E-mail address: andrzej.fertala@jefferson.edu (A. Fertala).
[1] These authors contributed equally to this work.

https://doi.org/10.1016/j.bone.2018.04.008
Received 14 November 2017; Received in revised form 10 April 2018; Accepted 12 April 2018
Available online 13 April 2018

efforts to prevent skeletal dysplasias, researchers need to develop an effective drug-, gene-, or cell-based therapy to block the expression of the mutant allele or to attenuate the effects imposed by mutant collagen molecules. It then needs to be determined whether this therapy must be applied during a specific time window in order to be effective. Furthermore, it must be shown whether any therapeutic effects are stable or transient.

While the first problem is beyond the realm of this study, we focused instead on determining the optimal time frame for the application of a model therapy and on studying the persistence of any effects. Specifically, to address the problem of the timing of therapy application, we utilized an inducible mouse model of mild SED caused by the R992C substitution in collagen II [4,18]. Because the mutant transgene may be switched off or on at any developmental stage in this model, we were able to study the consequences of stopping the expression of the mutant collagen II chains at the beginning of embryonic development and at various postnatal stages [4,18]. Our earlier studies thoroughly validated this model by demonstrating that growth plate's structure is altered when the mutant R992C collagen II is constantly expressed. Earlier studies further demonstrated that switching off the expression of the mutant collagen II chains at the beginning of embryonic growth blocks the SED phenotype [4]. Subsequently, we studied the consequences of switching off the R992C collagen II at birth and at later postnatal stages. Results of these studies indicated that the structure of cartilage and bone improved significantly only when the mutant molecules were blocked at birth, but not when blocked at later postnatal stages [18].

Here, we employ an inducible SED model to study the consequences of activating the R992C collagen II mutant postnatally in mice in which the expression of this mutant was at first blocked during the entire prenatal development.

2. Materials and methods

2.1. Mutation nomenclature

The R992C (p.R1192C) amino acid substitution is named according to the literature, with amino acid residues numbered from the first glycine residue of the collagen triple helix.

2.2. Transgenic mice

All mice received humane care according to the guidelines in the Guide for the Care and Use of Laboratory Animals. Procedures performed on animals were approved by the Thomas Jefferson University's Institutional Animal Care and Use Committee.

We employed a well-characterized transgenic mouse model of SED based on a DNA construct encoding procollagen II with the R992C substitution. In this model, the transgene is expressed conditionally, while the endogenous *Col2a1* gene is expressed constantly [4,18]. To enable a direct microscopic visualization of the expression patterns of the exogenous procollagen II, its pro-α chains were tagged at the C terminus with green fluorescent protein (GFP). As we demonstrated earlier, the GFP-tag does not interfere with functions of mature collagen II molecules because it is naturally cleaved off together with the C propeptides of the procollagen II-GFP chimeras [4,5,18]. GFP-tagged procollagen II molecules harboring the R992C mutation are referred to as R992C-ProII.

Although we described our model in detail elsewhere, here we present its key characteristics: (i) in addition to the DNA construct for the R992C-ProII mutant, the expression of tetracycline (Tet) transactivator (tTA) is maintained in the mice to enable Tet-dependent regulation of expression of the construct; (ii) the presence of cre recombinase, the expression of which is driven by a chondrocyte-specific promoter (Col2a1-cre), facilitates the chondrocyte-specific expression of the R992C-ProII transgene; (iii) the presence of all three transgenes (*i.e.*, for R992C-ProII; for tTA; and for Col2a1-cre) is needed to express the exogenous R992C-ProII protein; (iv) the expression of the R992C-ProII construct is only possible in the absence of doxycycline (Dox) while the expression is inhibited completely in the presence of Dox supplied in drinking water at 0.2 mg/ml; (v) triple-transgenic mice expressing R992C-ProII, together with tTA and Col2a1-cre, are described as mutant (MT); (vi) because of the genetics, not all littermates are positive for all three transgenes needed to produce R992C-ProII; transgenic mice that lack at least one of the required three transgene DNA constructs (*i.e.*, either for R992C-ProII, for tTA, or for Col2a1-cre) are named wild type (WT); in these mice, the exogenous R992C-ProII protein is not produced but the endogenous normal procollagen II is [4,18].

2.3. Identification of triple transgenes

Offspring generated *via* a breeding strategy described elsewhere were analyzed by PCR for the presence of all three transgenes [4,18].

2.4. Transgene expression and experimental groups

Initially, in the triple-transgene embryos (MT), the R992C-ProII was not produced during development because pregnant mothers were receiving Dox. This mutant was also not produced in WT members of the same developing litter that did not harbor all three transgenes. After birth, the Dox treatment was stopped to initiate the expression of the R992C-ProII in triple-transgene MT littermates. Thus, the triple-transgene mice in which the expression of the R992C-ProII was switched on only postnatally are referred to as MT-pON. The WT and MT-pON littermates were sacrificed at either 7-week or 10-week time points. We selected the 7-week time point to study defined features of the growth plates in growing bones, and the 10-week time point to analyze corresponding features in mature mouse bones [19–22].

We also utilized a control group of mice maintained constantly in the absence of Dox. In this group, the MT littermates harboring all three transgenes produced the R992C-ProII constantly (MT-cON), *i.e.* prenatally and postnatally, while the WT littermates missing at least one transgene did not produce this mutant at all [4,18].

The number of mice from each group available for specific assays is listed in Table 1. Note that the breeding protocol employed here was theoretically predicted to generate 12.5% triple-transgene MT offspring, and our earlier studies confirm this specific percentage [4].

2.5. Tissue harvesting and histology of growth plates

Mice were euthanized by CO_2 overdose. Before processing the mice for whole-skeleton staining with alizarin red and alcian blue, their right hind limbs were collected for histology. Subsequently, the hind paws were separated from the collected limbs. Next, the samples were fixed in a 4% solution of paraformaldehyde and decalcified in a solution of

Table 1
Summary of the growth plate measurements.

Genotype/Age	Number of mice	Average number of individual data points/mouse[a]		
		HZ	AC	BiP
MT-cON/7wks	7	25	10	10
MT-pON/7wks	3	29	3	7
WT/7wks	11	26	8	8
MT-cON/10wks	8	25	10	3
MT-pON/10wks	4	26	3	5
WT/10wks	12	33	8	4

[a] These numbers represent measurements done on various tissue sections and different regions of these sections. Symbols: HZ, hypertrophic zone; AC, articular cartilage; BiP, binding immunoglobulin protein.

14% EDTA, pH = 7.1, for two weeks in the dark [4,18]. Subsequently, the specimens were stained with hematoxylin and eosin (H&E) to visualize the general morphology and the cellularity. The tibia-femur complexes were also stained with Sirius red (Polysciences Inc., Warrington, PA) to visualize birefringent collagen fibrillar deposits in the polarized light (Eclipse LV100POL, Nikon Inc., Melville, NY).

2.6. Immunostaining of the growth plates

Tissue slices, 3- to 5-μm thick, of paraffin-embedded knee joints were processed for immunohistology, as described previously [4,18]. We analyzed the following antigens: (i) collagen X, a structural element of the hypertrophic zone; (ii) collagen VI, a structural protein present in the pericellular zone; (iii) GFP, to detects GFP-tagged R992C-ProII; (iv) acetylated tubulin, a component of primary cilia; and (v) binding immunoglobulin protein (BiP), a chaperone protein whose increased expression is an indicator of ER stress. Specific primary and secondary antibodies and procedures employed to visualize collagen IV, collagen X, acetylated tubulin, and BiP are described in detail in earlier studies [4,18]. Here, to detect GFP we employed the rabbit polyclonal anti-GFP antibody (Santa Cruz Biotechnology, Dallas, TX). Subsequently, the binding of this antibody to intracellular GFP was detected with a secondary antibody conjugated to a red-fluorophore Alexa Fluor 594 (Molecular Probes, Thermo Fisher Scientific Inc., Waltham, MA).

All assays included negative controls in which primary antibodies against specific antigens were not used. A microscope (Eclipse E600, Nikon, Inc.), equipped with a monochrome digital camera (DS-Qi1Mc, Nikon, Inc.), was employed to observe immunostained specimens.

2.7. Image analyses

The microscopic assays focused on the tibial growth plates. Microscopic images were processed using the NIS Elements software (Nikon, Inc.). For specimens stained with fluorophores, we collected a sequence of images of consecutive focal planes along the *Z*-axes of the analyzed areas. Subsequently, these sequences were processed with the Extended Depth Focus module of the NIS Elements software (version Ar 4.5, Nikon, Inc.) to fully utilize in-focus information of the analyzed region of interest (ROI). A minimum of three sections from each analyzed specimen was prepared. Subsequently, defined parameters (see below) were measured in relevant areas. Table 1 presents detailed information on the number of data points for each group and a parameter.

2.8. Hypertrophic zones (HZ)

The height of the HZ seen in H&E-stained specimens was measured using the NIS Elements software and also identified by the presence of collagen X in corresponding tissue sections, as described [18].

2.9. Acellular areas (AC)

The acellular regions surrounding groups of chondrocytes present in the tibial growth plates were readily distinguishable in the Sirius red-stained specimens observed with a polarizing microscope. The acellular areas were measured and then expressed as a percent of the total area of the analyzed ROI, as described [18].

2.10. Assays of BiP

The expression of BiP was analyzed by measuring the pixel intensities of the BiP-positive signals from growth plate chondrocytes. All analyzed sections were processed at the same time to ensure an identical condition of the BiP-specific immunostaining. Following the staining, we photographed the BiP-positive chondrocytes; all images were acquired with identical camera settings. In each sample, the mean intensity of BiP-specific pixels seen in the viewing areas was measured using the NIS Elements software.

2.11. Morphometry of bones

The skeletal indices of the femora, tibiae, and skulls of 10-week-old mice stained with alizarin red and alcian blue were measured with a digital caliper to 0.01 mm (Absolute Digimatic Caliper, Mitutoyo Corporation, Kawasaki-shi, Japan), as described [4,18]. The following parameters were recorded: (i) for the femora: the femoral length, the condylar, and the midshaft widths; (ii) for the tibiae: the tibia length and the condylar, the midshaft, and the malleolar widths; and (iii) for the skulls: the length measured from the tip of the nasal bone to the back of the occipital bone, the width measured at the widest point of the parietal bone, and the inner canthal distances. Subsequently, the length:mean-of-widths ratios were calculated to compare the shapes of the analyzed skeletal elements, as described [4,18]. When comparing potential changes in the mutant mice with the relevant control group, a relatively small ratio would indicate a disproportionately shorter and wider bone.

2.12. Data analysis

For histology-based assays of growth plates, we collected data from individual tissue sections derived from the MT-pON, MT-cON, and WT mice. Specifically, we measured the average height of the HZ, the percent of area of the growth plates occupied by the AC, and the mean pixel intensity of the BiP-positive signals. Detailed procedures for measuring these parameters were described previously [18]. A two-way ANOVA with Tukey *post hoc* tests was run to examine interaction of age effects and genotype (WT, MT-pON, MT-cON) effects on HZ, AC, or BiP and was considered to be significant at $p < 0.05$ (SPSS Statistics, version 24, IBM). Due to a relatively small number of samples available for the morphometry of bones, we report individual data points and the means with 95% confidence intervals (CI) for each analyzed group, as described in our earlier study [18].

3. Results

3.1. Transgenic mice and activation of the expression of the R992C mutant

In all assays, the MT mice and their WT littermates were readily identified by PCR for the R992C-ProII, tTA, and Col2a1-cre constructs [4,18]. Consistent with our earlier studies, postnatal activation of the expression of the R992C-ProII construct was confirmed in the MT-pON mice by observing the presence of the GFP-specific signals in chondrocytes (Fig. 1) [4,18]. Note that based on our earlier detailed studies done on the chondrocytes of the MT mice, we expect that a full expression of the R992C-ProII has occurred within 48 h following stopping the Dox supply [4].

To avoid potential problems with the time-dependent decay of the GFP-specific fluorescence and with “green” autofluorescence of analyzed tissues, here, we utilized the anti-GFP antibody to detect the R992C-ProII. As indicated in Fig. 1, the apparent intensities of specific signals in the growth plates and articular cartilage of 7-week old mice from the MT-cON and MT-pON groups were similar. Comparable intensities in corresponding groups of 10-week old mice were also observed (not shown). Consistent with published studies, the intensities of intracellular signals from the R992C-ProII construct expressed under indirect control of the Col2a1 promoter was not uniform along stacks of chondrocytes (Fig. 1) [23,24].

3.2. Morphology of the growth plates

As demonstrated earlier, chondrocytes present in the growth plates of the MT-cON mice from the 7-week-old and 10-week-old groups were disorganized and did not form well-defined columns. Moreover, the

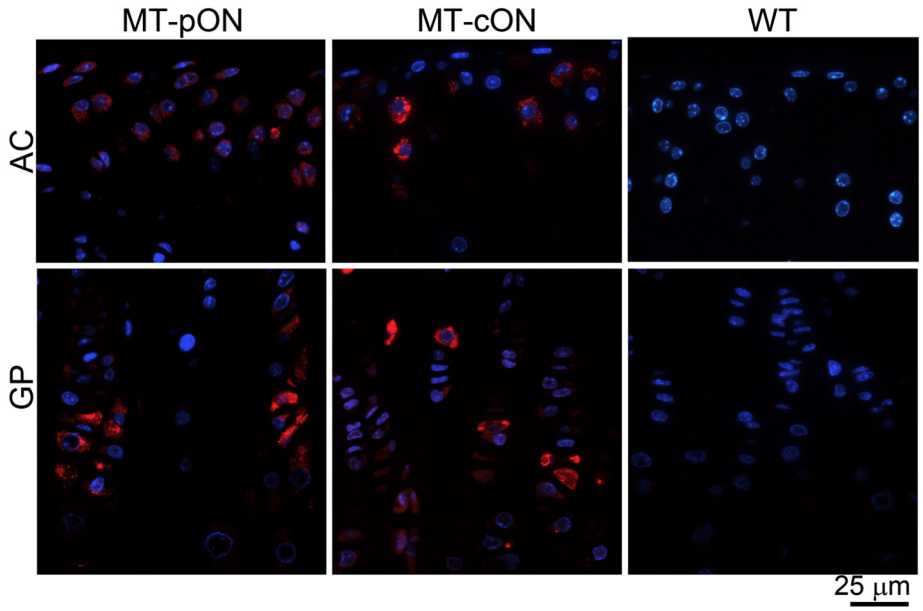

Fig. 1. Visualization of the distribution of the R992C-Pro II-positive cells in articular cartilage (AC) and growth plates (GF) in the 7-week-old mice.

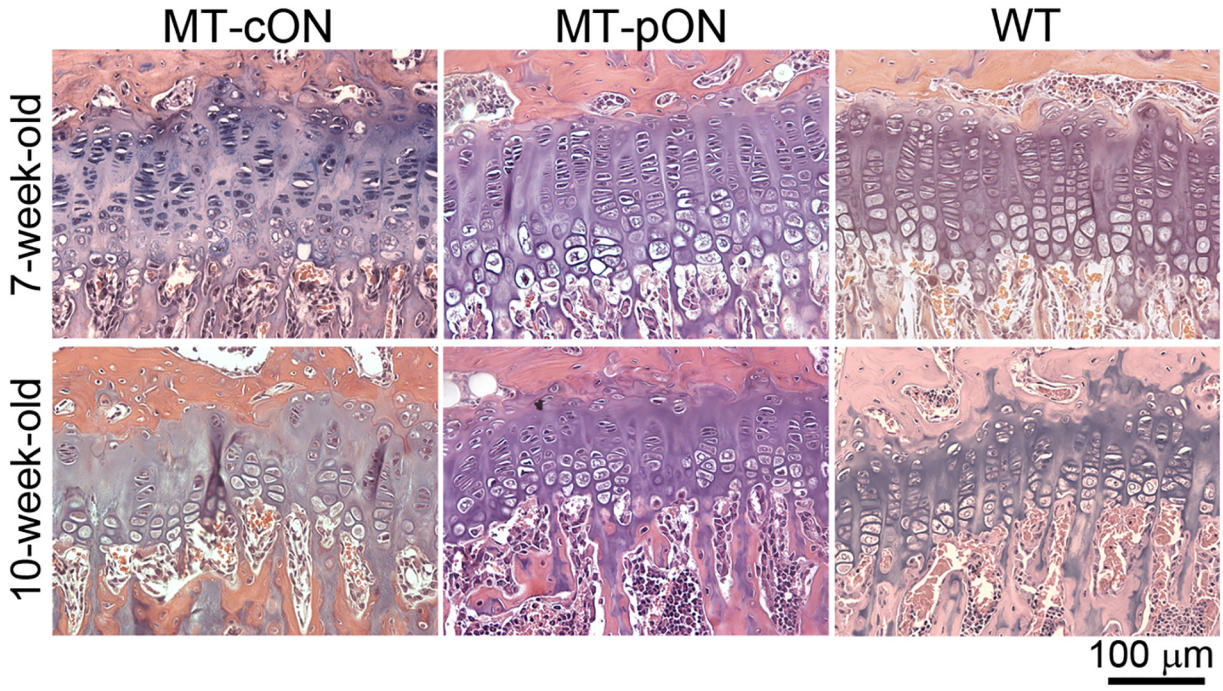

Fig. 2. The general morphology of tibial growth plates of mice from the 7-week-old and 10-week-old groups.

acellular areas in the growth plates of these mice increased in comparison to their WT littermates (Figs. 2 & 3) [18]. In contrast, in the 7-week-old and 10-week-old MT-pON mice, the morphology of the growth plates was similar to that of their WT littermates (Fig. 2).

3.3. Hypertrophic zones

In our earlier studies, we demonstrated that the height of the HZ was reduced in the growth plates of the MT-cON mice [18]. Here, we also measured the height of these zones as a parameter for describing potential growth plate changes due to postnatal activation of the R992C-ProII mutant. We observed a significant interaction between the effects of age and genotype on the heights of HZ, $F(2, 1100) = 95.5$, $p < 0.0001$. The simple main effects analysis showed that age had a significant reducing effect on the height of the HZ ($p < 0.0001$). Similarly, the genotype had a significant reducing effect on the height of HZ ($p < 0.0001$). Fig. 3 illustrates these changes for each age and genotype group.

3.4. Area of the acellular space of growth plates

As an additional parameter, we also measured the percentage of the AC area to determine any organizational changes in the growth plates resulting from switching on the expression of the R992C-ProII (Fig. 3). We demonstrated that there was a significant interaction between the effects of age and genotype on the percentage of the AC area, $F(2, 341) = 26.4$, $p < 0.0001$. The simple main effects analysis showed that age ($p < 0.0001$) and genotype ($p < 0.0001$) both had a significant

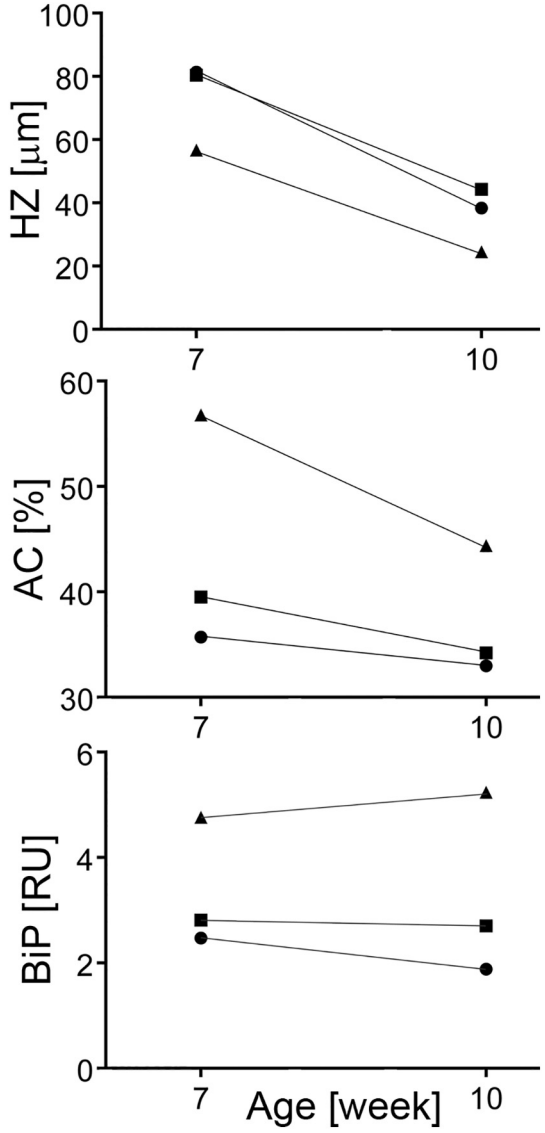

Fig. 3. The plots of the means of the HZ, AC, and BiP parameters for each combination of age and genotype groups plotted as line graphs. Symbols: WT (●), MT-cON (▲), MT-pON (■).

effects on changing the percentage of the AC area in analyzed growth plates. Fig. 3 illustrates these changes for individual age and genotype groups.

3.5. Expression of BiP

The BiP-positive chondrocytes were readily apparent in the growth plates of analyzed mice (Fig. 4). When we measured the pixel intensities of the BiP-positive signals, we found that the there was no a significant interaction between the effects of age and genotype of mice on the pixel intensities of the BiP-specific signals from growth plate chondrocytes, F (2, 2.7), $p = 0.072$. The simple main effects analysis showed that age did not have a significant effect on the pixel intensity of the BiP-specific signals ($p = 0.074$). In contrast, a significant increasing effect of genotype was observed on the BiP pixel intensity ($p < 0.0001$). Fig. 3 illustrates these effects for individual age and genotype groups.

3.6. Pericellular matrix

We studied how switching on the expression of the R992C-ProII at birth affected the organization of the pericellular matrix. Specifically, we analyzed the distribution of collagen VI in articular cartilage and growth plates (Fig. 5). We found that, similar to control, collagen VI was present in well-defined pericellular zones in both the 7-week-old and 10-week-old groups of the MT-pON mice (Fig. 5). In contrast, in the MT-cON mice in which the mutant collagen II chains were expressed throughout all developmental stages, we found diffuse distribution of collagen VI around chondrocytes in the articular cartilage (Fig. 5). Intracellular localization of collagen VI was also apparent in these mice. We reported similar alterations of collagen VI distribution in these mice in earlier studies [18].

3.7. Arrangement of primary cilia

In properly organized growth plates, the primary cilia of chondrocytes align along the longitudinal axis of long bones [4,25–28]. As demonstrated by us earlier, in the MT-cON mice cilia do not align properly due to disorganization of growth plates chondrocytes [4]. In contrast, as illustrated in Fig. 6, in all MT-pON mice in which the expression of the R992C-ProII mutant was switched on at birth, chondrocytes in the growth plates were properly aligned regularly. Similar alignment was observed in WT littermates in which the collagen II mutant was not expressed at any stage of skeletal growth.

3.8. Morphometry of bones

We measured selected indices of bones from the 10-week-old WT and MT-pON mice. Table 2 presents results of these measurements.

To compare the shapes of the analyzed skeletal elements, we also calculated the length:mean-of-widths ratios; a relatively small ratio indicated a disproportionately shorter bone [4,18]. Performing similar measurements, in our earlier studies, we demonstrated a significant shortening of femora, tibiae, and skulls of the 10-week-old MT-cON mice [4]. To compare these earlier results, here, we measured these indices for the femora, tibiae, and skulls of the 10-week-old MT-pON mice and their WT littermates. Although the ratios for the femora and tibiae trended slightly lower in the MT-pON mice compared to their WT littermates, we observed a slight upward trend for the length:mean-of-widths ratio calculated for the skulls (Fig. 7).

4. Discussion

Our earlier studies indicated that aberrant growth plates developed in the presence of the R992C-ProII mutant have a limited ability to remodel after the expression of this mutant is switched off postnatally [18]. In the research presented here, we switched off the expression of the R992C-ProII mutant during the entire embryonic development and analyzed whether the postnatal activation of the expression of the mutant alters the architecture of growth plates of growing bones.

A couple conditions have to be met to render this model functional: (i) the first condition is that stopping Dox treatment will readily activate the expression of the R992C-ProII mutant and (ii) the second condition is that the amounts of R992C-ProII produced at 7-week-old and 10-week-old time points in the MT-pON mice are comparable with those produced at the corresponding time points in the MT-cON mice.

We know that the first condition is met based on our published detailed experiments done on chondrocytes, isolated from the mutant mice [4]. In brief, utilizing cultures of these chondrocytes we demonstrated that the expression system we employed reacts to Dox within 48 h of changing the Dox status. For instance, adding Dox to cell cultures of chondrocytes stops the production of the mutant completely within 48 h. Similarly, full production of the mutant is achieved at the same time after removing Dox from cell culture media. Although these observations had to be done in cell culture conditions because we cannot do similar observations at the cell level in living mice, we argue that similar dynamics exist *in vivo*. We base this argument on the *in vivo*

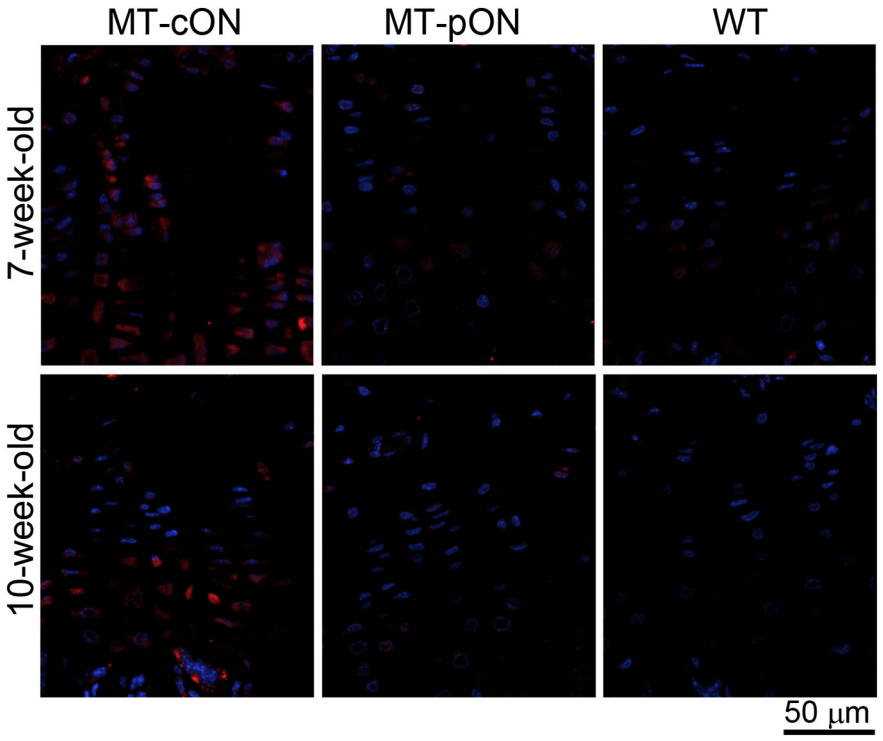

Fig. 4. BiP positive staining in the growth plates of the mutant and control mice.

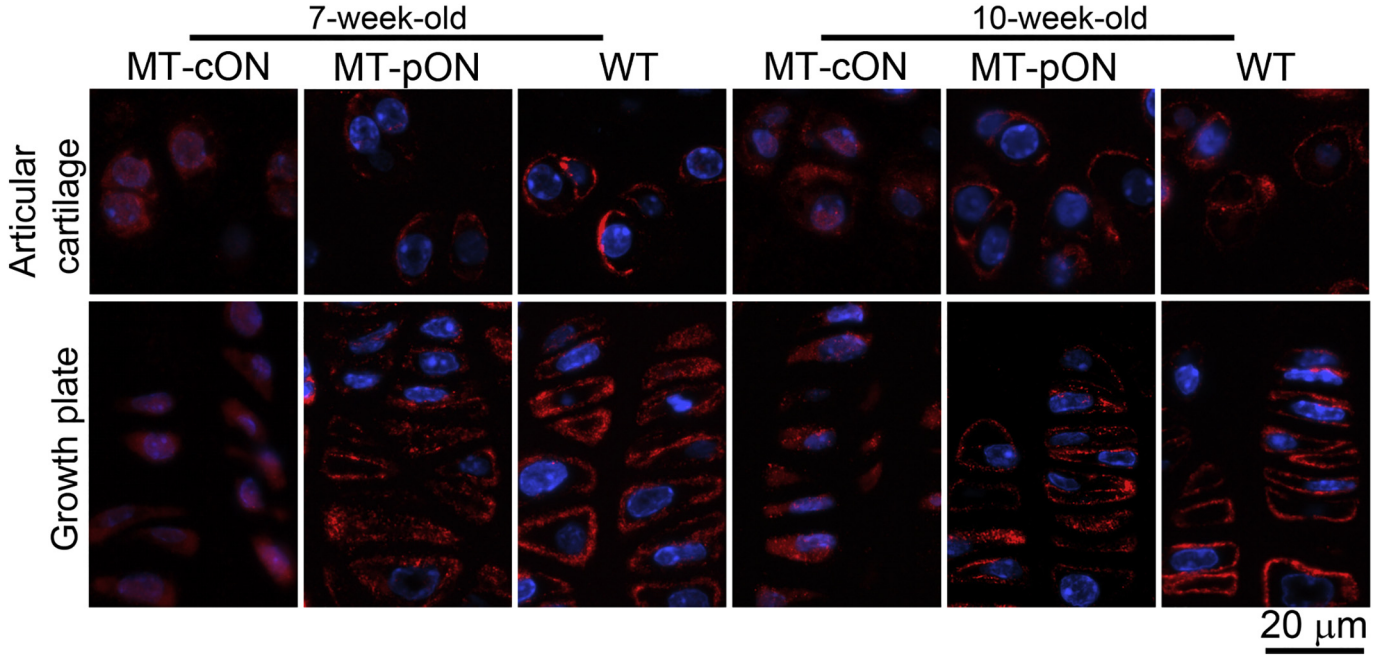

Fig. 5. Immunostaining of collagen VI in 7-week-old and 10-week-old mice.

studies in mice demonstrating that upon removal of Dox, like in the system we used here, activation of Tet-regulated transgenes in a number of tissues and organs occurs after 24 h [29]. Considering that we achieve a full inhibition of our transgene expression during embryo development with a relatively low Dox concentration of 0.2 mg/ml, we expect rather fast clearance of this antibiotic, thus prompt activation of the transgene [18]. A relatively short half-life (2.8 h) of Dox in mice further suggests the prompt activation of the expression of the R992C-ProII upon stopping the Dox supply [30,31]. Employing our experimental model, we are not able to pin point the exact starting point of the postnatal expression of R992C-ProII. Still considering the above characteristics of Dox and the Tet-regulated expression systems, we speculate that following Dox removal, the expression of our mutant starts within 24 h and reaches its full potential within another 48 h. Following this initial period, the ECM formation and remodeling occurs in the constant presence of the R992C-ProII mutant.

We demonstrated that our model also fulfills the second condition. Specifically, we demonstrated that at the protein level the expression of the R992C-ProII mutant in the MT-pON and the MT-cON mice is comparable.

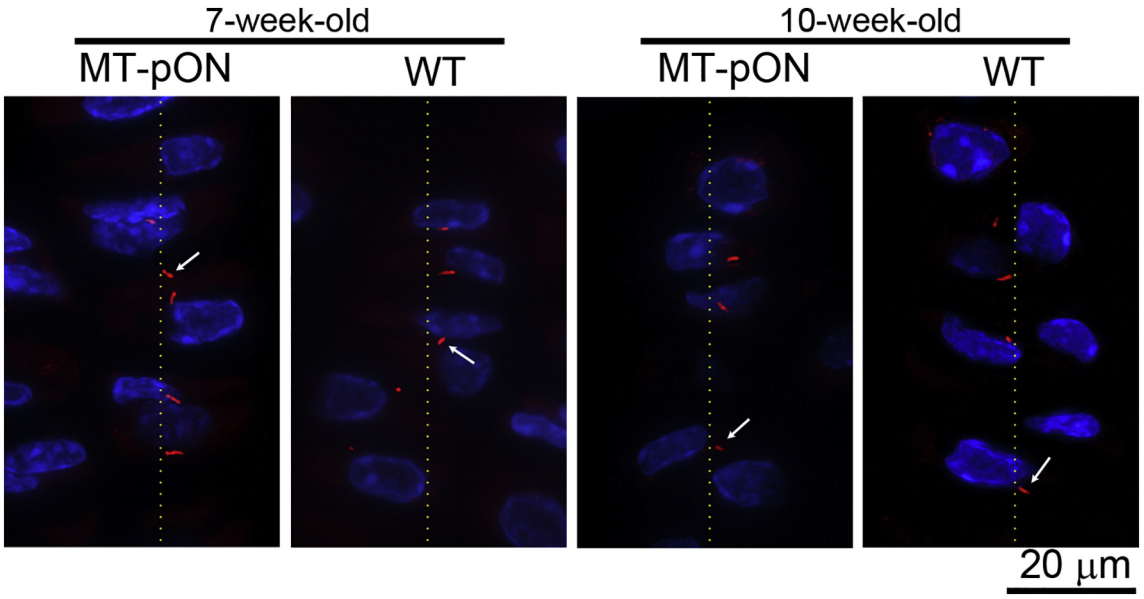

Fig. 6. Acetylated tubulin-specific immunostaining of primary cilia in chondrocytes of 7-week-old and 10-week-old mice. Dotted lines approximate the long axis of the analyzed tibiae. Arrows indicate positions of selected primary cilia.

Table 2
Measurements of bone indices in 10-week-old mice.

Bone indices	WT $n = 12$	MT-pON $n = 4$
	Mean ± S.D. [mm]	Mean ± S.D. [mm]
Femoral length	15.06 ± 0.51	14.31 ± 0.49
Femoral condylar width	2.85 ± 0.09	2.89 ± 0.04
Femoral midshaft width	1.85 ± 0.12	1.83 ± 0.04
Tibial length	17.48 ± 0.47	16.83 ± 0.25
Tibial condylar width	3.19 ± 0.08	3.14 ± 0.08
Tibial midshaft width	1.10 ± 0.12	1.02 ± 0.02
Tibial malleolar width	2.66 ± 0.17	2.57 ± 0.08
Skull length	23.08 ± 0.73	22.26 ± 0.37
Inner canthal distance	5.11 ± 0.93	3.89 ± 0.02
Skull width	10.59 ± 0.19	10.16 ± 0.05

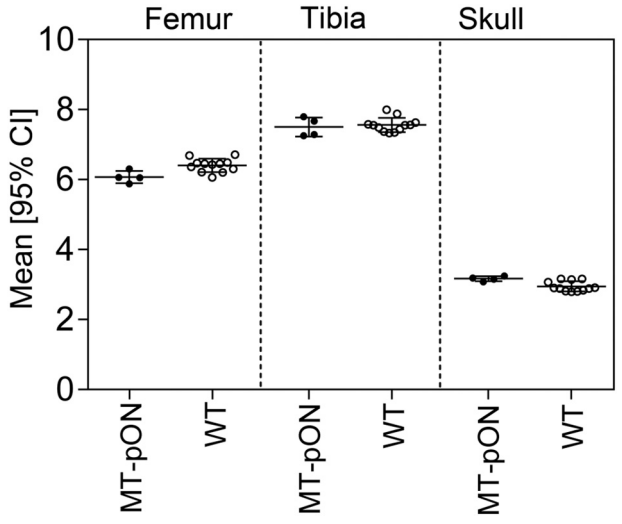

Fig. 7. A graphic representation of the length:mean-of-widths ratios of femora, tibiae, and skulls of the 10-week-old mice. The individual data points and the means with 95% CI are presented.

A fundamental parameter indicating the proper cartilaginous architecture of growing endochondral bones is the correct columnar organization of the growth plate chondrocytes. This organization depends on a well-formed collagen II-based scaffold that serves as the core of a complex guiding platform needed for the proper spatial positioning of chondrocytes. Studies demonstrated that specific receptors including integrins, discoidin domain receptors, NG2, CD44, and annexin 5, play a vital role in this positioning [32]. Even though these receptors are present on the entire surface of the chondrocyte cell membrane, the α2, α3, and β1 integrins as well as NG2 are also located on primary cilia [33]. By interacting with elements of the extracellular matrix (ECM), primary cilia play a critical role in sensing mechanical cues from the cartilaginous environment and guiding the organization of the chondrocytes [25,26,34,35].

Our earlier studies demonstrated that aberrant ECM formed in the MT-cON mice alters the function of primary cilia and leads to disorganization of the chondrocytes. These studies also demonstrated that in the absence of the R992C collagen II mutant, the primary cilia function correctly, allowing normal columnar organization of growth plate chondrocytes [4]. Thus, the demonstration of a correct distribution of the primary cilia and normal arrangement of chondrocytes in the MT-pON mice suggests that the cartilaginous ECM has a proper architecture. The stability of the architectural features of the cartilage in these mice was further evident by the observation that, in contrast to the MT-cON mice, switching on the expression of the R992C-ProII postnatally causes no major changes in the height of the HZ or in the percentage of the AC areas that separate the columns of chondrocytes.

Switching on the expression of the R992C-ProII at birth did not greatly affect the collagen II-based architecture and did not substantially impact the organization of other elements of the cartilaginous matrix. For instance, postnatal expression of the mutant did not change the architecture of the collagen VI-rich pericellular matrix that facilitates communication between the chondrocyte and the collagen II-rich interterritorial ECM [36,37]. In contrast, we demonstrated an abnormal pattern of distribution of collagen VI in the MT-cON mice expressing the R992C collagen II mutant constantly [18].

The ultimate evidence for the stability of collagenous matrices formed during embryonic development, despite the postnatal expression of the R992C-ProII mutant, was our observation of the normal growth of long bones and the skulls of the MT-pON mice. This observation is in contrast with our earlier studies on the MT-cON mice, in which we demonstrated significant changes in the shape of bones in comparison to WT littermates [4].

Our demonstration of the stability of the cartilaginous blueprint formed during embryonic development is consistent with a recently published study that showed that correct fibrillar architecture and mechanical strength of the interterritorial and pericellular collagenous matrices facilitate a proper columnar arrangement of growth plate chondrocytes [38]. This study also found that formation of collagen fibrils, the cornerstone of the interterritorial and pericellular matrices, starts on day E13.5 and is completed when mice reach 2 weeks of age, after which neither major changes in fibrillar architecture nor in the mechanical properties of the collagenous matrices take place.

Our results demonstrating the correct structure of the growth plates in the MT-pON mice corroborate earlier observations on the role of well-organized collagen II-rich matrices for the development of epiphyseal growth plates. Prior studies on mice with targeted inactivation of the *Col2a1* gene showed that the presence of collagen II is not necessary to signal the development of the endoskeleton or for the formation of long bones, and moreover, well-organized cartilage is not needed for the initial mineralization of long bones or for the synthesis of periosteal bone [39]. In contrast, these earlier studies demonstrated that the presence of well-organized cartilage is essential for the formation and growth of the epiphyseal growth plates of long bones. Specifically, these studies showed that transgenic mice with inactivated *Col2a1* have completely disorganized growth plates and have no zonal arrangement of chondrocytes [39].

When we studied the consequences of the postnatal expression of the R992C-ProII mutant on ER stress, we were somewhat surprised to find that the expression of BiP, a marker of the cellular stress, was not increased significantly in the MT-pON mice, despite the expression of the R992C-ProII postnatally. In contrast, the expression of BiP significantly increased in the MT-cON mice when compared to WT control. These results may suggest that coping with ER stress caused by the excessive intracellular accumulation of misfolded collagen II chains may not only depend upon an effective intracellular mechanism of unfolded protein response, but also on the proper ECM structure. Previously published research supports the notion that the presence of proper ECM can change the response of chondrocytes to ER stress and thereby reduce apoptosis [40]. That research demonstrated that in well-developed ECM, the concentration of cellular stressors needed to be relatively high in order to increase the ER stress and production of BiP in chondrocytes. In contrast, to trigger ER stress and increase the BiP production in chondrocytes grown with poor-developed ECM, the concentration of cellular stressors needed to be relatively low [40].

Our current findings, in combination with our earlier findings, demonstrate that switching off the expression of the R992C-ProII mutant from the very beginning of embryonic development or in newborn mice, but not later, produces a normal skeletal phenotype These findings suggest a few important conclusions: (i) these studies indicate that therapeutic approaches for targeting heritable skeletal dysplasias caused by mutations in collagen II may be effective if they aim to block the onset of pathological changes rather than repair established aberrations; (ii) these studies indicate the need for early therapeutic interventions during embryonic development; and (iii) they suggest that early interventions to eliminate or reduce the amount of the mutant collagen II molecules may offer stable effects. The conclusion that early therapeutic intervention is needed to reduce the effects of mutations in collagen II is consistent with observations from studies on other heritable diseases of connective tissues, including achondrodysplasia caused by mutations in the fibroblast growth factor receptor 3 gene (*Fgfr3*) and Alport syndrome caused by the absence of the collagen α3(IV) chain [11,41].

Since mutations in collagen II cause a broad spectrum of consequences, ranging from embryonic lethal to mild forms of SED, it is not clear if early therapeutic interventions are needed to achieve positive outcomes for all cases of SED. However, considering that the R992C mutation causes the mild form of SED and that therapeutic effects were achieved only after switching off the expression of the mutant at the early developmental stages, we postulate that early intervention may be required for all cases of SED. Thus, therapeutic approaches are needed that effectively target the expression of mutant alleles during prenatal stages, as are diagnostic tools that are able to detect collagen II mutations at early developmental stages.

Our study has a couple limitations. First, the number of samples available for morphometry of bones was limited because only 12.5% of littermates expressed the three transgenes needed for the production of the R992C mutant [4,18]. Thus, although we observed no major differences between the MT-pON and WT mice, the statistical significance of the results could not be clearly determined. Second, we did not establish the exact time point of switching on the expression of R992C-ProII following postnatal Dox removal. Third, since strict correlations between mice and human developmental time lines do not exist, based on this study we cannot clearly draw parallels between observations done with the model mutant mice and potential changes in patients harboring mutations in the *COL2A1*. Still, this study suggests that future therapies of skeletal dysplasias applied at early developmental stages may offer long-term positive effects that could persist even in the presence of mutant molecules expressed postnatally.

Acknowledgement

This research did not receive any specific grant from funding agencies in the public, commercial, or not-for-profit sectors. The authors thank Jennifer Fisher Wilson for revising the article.

References

[1] W.V. Arnold, A. Fertala, Skeletal diseases caused by mutations that affect collagen structure and function, Int. J. Biochem. Cell Biol. 45 (8) (2013) 1556–1567.
[2] M. Barat-Houari, G. Sarrabay, V. Gatinois, A. Fabre, B. Dumont, D. Genevieve, I. Touitou, Mutation update for COL2A1 gene variants associated with type II collagenopathies, Hum. Mutat. 37 (1) (2016) 7–15.
[3] W. Arnold, A. Fertala, Extracellular matrix and collagen disorders, in: L. Cannada (Ed.), Orthopaedic Knowledge Update, American Academy of Orthopaedic Surgeons, 2014, pp. 223–236.
[4] M. Arita, J. Fertala, C. Hou, A. Steplewski, A. Fertala, Mechanisms of aberrant organization of growth plates in conditional transgenic mouse model of spondyloepiphyseal dysplasia associated with the R992C substitution in collagen II, Am. J. Pathol. 185 (1) (2015) 214–229.
[5] H. Ito, E. Rucker, A. Steplewski, E. McAdams, R.J. Brittingham, T. Alabyeva, A. Fertala, Guilty by association: some collagen II mutants alter the formation of ECM as a result of atypical interaction with fibronectin, J. Mol. Biol. 352 (2) (2005) 382–395.
[6] A. Fertala, A.L. Sieron, E. Adachi, S.A. Jimenez, Collagen II containing a Cys substitution for Arg-alpha1-519: abnormal interactions of the mutated molecules with collagen IX, Biochemistry 40 (48) (2001) 14422–14428.
[7] V. Hintze, A. Steplewski, H. Ito, D.A. Jensen, U. Rodeck, A. Fertala, Cells expressing partially unfolded R789C/p.R989C type II procollagen mutant associated with spondyloepiphyseal dysplasia undergo apoptosis, Hum. Mutat. 29 (6) (2008) 841–851.
[8] K.L. Posey, J.T. Hecht, Novel therapeutic interventions for pseudoachondroplasia, Bone 102 (2017) 60–68.
[9] L.L. Tosi, M.L. Warman, Mechanistic and therapeutic insights gained from studying rare skeletal diseases, Bone 76 (2015) 67–75.
[10] H. Kanazawa, H. Tanaka, M. Inoue, Y. Yamanaka, N. Namba, Y. Seino, Efficacy of growth hormone therapy for patients with skeletal dysplasia, J. Bone Miner. Metab. 21 (5) (2003) 307–310.
[11] A. Yamashita, M. Morioka, H. Kishi, T. Kimura, Y. Yahara, M. Okada, K. Fujita, H. Sawai, S. Ikegawa, N. Tsumaki, Statin treatment rescues FGFR3 skeletal dysplasia phenotypes, Nature 513 (7519) (2014) 507–511.
[12] E.M. Horwitz, D.J. Prockop, P.L. Gordon, W.W. Koo, L.A. Fitzpatrick, M.D. Neel, M.E. McCarville, P.J. Orchard, R.E. Pyeritz, M.K. Brenner, Clinical responses to bone marrow transplantation in children with severe osteogenesis imperfecta, Blood 97 (5) (2001) 1227–1231.
[13] E.M. Horwitz, D.J. Prockop, L.A. Fitzpatrick, W.W. Koo, P.L. Gordon, M. Neel, M. Sussman, P. Orchard, J.C. Marx, R.E. Pyeritz, M.K. Brenner, Transplantability and therapeutic effects of bone marrow-derived mesenchymal cells in children with osteogenesis imperfecta, Nat. Med. 5 (3) (1999) 309–313.
[14] E.M. Horwitz, P.L. Gordon, W.K. Koo, J.C. Marx, M.D. Neel, R.Y. McNall, L. Muul, T. Hofmann, Isolated allogeneic bone marrow-derived mesenchymal cells engraft and stimulate growth in children with osteogenesis imperfecta: implications for cell therapy of bone, Proc. Natl. Acad. Sci. U. S. A. 99 (13) (2002) 8932–8937.
[15] K. Le Blanc, C. Gotherstrom, O. Ringden, M. Hassan, R. McMahon, E. Horwitz, G. Anneren, O. Axelsson, J. Nunn, U. Ewald, S. Norden-Lindeberg, M. Jansson, A. Dalton, E. Astrom, M. Westgren, Fetal mesenchymal stem-cell engraftment in

bone after in utero transplantation in a patient with severe osteogenesis imperfecta, Transplantation 79 (11) (2005) 1607–1614.
[16] C. Gotherstrom, M. Westgren, S.W. Shaw, E. Astrom, A. Biswas, P.H. Byers, C.N. Mattar, G.E. Graham, J. Taslimi, U. Ewald, N.M. Fisk, A.E. Yeoh, J.L. Lin, P.J. Cheng, M. Choolani, K. Le Blanc, J.K. Chan, Pre- and postnatal transplantation of fetal mesenchymal stem cells in osteogenesis imperfecta: a two-center experience, Stem Cells Transl. Med. 3 (2) (2014) 255–264.
[17] J.K. Chan, C. Gotherstrom, Prenatal transplantation of mesenchymal stem cells to treat osteogenesis imperfecta, Front. Pharmacol. 5 (2014) 223.
[18] M. Arita, J. Fertala, C. Hou, J. Kostas, A. Steplewski, A. Fertala, Prospects and limitations of improving skeletal growth in a mouse model of spondyloepiphyseal dysplasia caused by R992C (p.R1192C) substitution in collagen II, PLoS One 12 (2) (2017) e0172068.
[19] J.M. Somerville, R.M. Aspden, K.E. Armour, K.J. Armour, D.M. Reid, Growth of C57BL/6 mice and the material and mechanical properties of cortical bone from the tibia, Calcif. Tissue Int. 74 (5) (2004) 469–475.
[20] M.D. Brodt, C.B. Ellis, M.J. Silva, Growing C57Bl/6 mice increase whole bone mechanical properties by increasing geometric and material properties, J. Bone Miner. Res. 14 (12) (1999) 2159–2166.
[21] M.G. Chambers, T. Kuffner, S.K. Cowan, K.S. Cheah, R.M. Mason, Expression of collagen and aggrecan genes in normal and osteoarthritic murine knee joints, Osteoarthr. Cartil. 10 (1) (2002) 51–61.
[22] M. Kveiborg, R. Albrechtsen, L. Rudkjaer, G. Wen, K. Damgaard-Pedersen, U.M. Wewer, ADAM12-S stimulates bone growth in transgenic mice by modulating chondrocyte proliferation and maturation, J. Bone Miner. Res. 21 (8) (2006) 1288–1296.
[23] M. Chen, A.C. Lichtler, T.J. Sheu, C. Xie, X. Zhang, R.J. O'Keefe, D. Chen, Generation of a transgenic mouse model with chondrocyte-specific and tamoxifen-inducible expression of Cre recombinase, Genesis 45 (1) (2007) 44–50.
[24] M.A. Tryfonidou, G.P. Lunstrum, K. Hendriks, F.M. Riemers, R. Wubbolts, H.A. Hazewinkel, C.R. Degnin, W.A. Horton, Novel type II collagen reporter mice: new tool for assessing collagen 2alpha1 expression in vivo and in vitro, Dev. Dyn. 240 (3) (2011) 663–673.
[25] S.R. McGlashan, C.J. Haycraft, C.G. Jensen, B.K. Yoder, C.A. Poole, Articular cartilage and growth plate defects are associated with chondrocyte cytoskeletal abnormalities in Tg737orpk mice lacking the primary cilia protein polaris, Matrix Biol. 26 (4) (2007) 234–246.
[26] B. Song, C.J. Haycraft, H.S. Seo, B.K. Yoder, R. Serra, Development of the post-natal growth plate requires intraflagellar transport proteins, Dev. Biol. 305 (1) (2007) 202–216.
[27] C.A. Poole, C.G. Jensen, J.A. Snyder, C.G. Gray, V.L. Hermanutz, D.N. Wheatley, Confocal analysis of primary cilia structure and colocalization with the Golgi apparatus in chondrocytes and aortic smooth muscle cells, Cell Biol. Int. 21 (8) (1997) 483–494.
[28] P. Satir, S.T. Christensen, Overview of structure and function of mammalian cilia, Annu. Rev. Physiol. 69 (2007) 377–400.
[29] A. Kistner, M. Gossen, F. Zimmermann, J. Jerecic, C. Ullmer, H. Lubbert, H. Bujard, Doxycycline-mediated quantitative and tissue-specific control of gene expression in transgenic mice, Proc. Natl. Acad. Sci. U. S. A. 93 (20) (1996) 10933–10938.
[30] R. Bocker, C.J. Estler, M. Maywald, D. Weber, Comparison of distribution of doxycycline in mice after oral and intravenous application measured by a high-performance liquid chromatographic method, Arzneimittelforschung 31 (12) (1981) 2116–2117.
[31] R. Bocker, L. Warnke, C.J. Estler, Blood and organ concentrations of tetracycline and doxycycline in female mice. Comparison to males, Arztl. Forsch. 34 (4) (1984) 446–448.
[32] A. Woods, G. Wang, F. Beier, Regulation of chondrocyte differentiation by the actin cytoskeleton and adhesive interactions, J. Cell. Physiol. 213 (1) (2007) 1–8.
[33] S.R. McGlashan, C.G. Jensen, C.A. Poole, Localization of extracellular matrix receptors on the chondrocyte primary cilium, J. Histochem. Cytochem. 54 (9) (2006) 1005–1014.
[34] C.J. Haycraft, R. Serra, Cilia involvement in patterning and maintenance of the skeleton, Curr. Top. Dev. Biol. 85 (2008) 303–332.
[35] C. Huber, V. Cormier-Daire, Ciliary disorder of the skeleton, Am. J. Med. Genet. C: Semin. Med. Genet. 160C (3) (2012) 165–174.
[36] C.A. Poole, M.H. Flint, B.W. Beaumont, Chondrons in cartilage: ultrastructural analysis of the pericellular microenvironment in adult human articular cartilages, J. Orthop. Res. 5 (4) (1987) 509–522.
[37] C.A. Poole, S. Ayad, R.T. Gilbert, Chondrons from articular cartilage. V. Immunohistochemical evaluation of type VI collagen organisation in isolated chondrons by light, confocal and electron microscopy, J. Cell Sci. 103 (Pt 4) (1992) 1101–1110.
[38] C. Prein, N. Warmbold, Z. Farkas, M. Schieker, A. Aszodi, H. Clausen-Schaumann, Structural and mechanical properties of the proliferative zone of the developing murine growth plate cartilage assessed by atomic force microscopy, Matrix Biol. 50 (2016) 1–15.
[39] S.W. Li, D.J. Prockop, H. Helminen, R. Fassler, T. Lapvetelainen, K. Kiraly, A. Peltarri, J. Arokoski, H. Lui, M. Arita, et al., Transgenic mice with targeted inactivation of the Col2 alpha 1 gene for collagen II develop a skeleton with membranous and periosteal bone but no endochondral bone, Genes Dev. 9 (22) (1995) 2821–2830.
[40] A.E. Nugent, D.L. McBurney, W.E. Horton Jr., The presence of extracellular matrix alters the chondrocyte response to endoplasmic reticulum stress, J. Cell. Biochem. 112 (4) (2011) 1118–1129.
[41] X. Lin, J.H. Suh, G. Go, J.H. Miner, Feasibility of repairing glomerular basement membrane defects in Alport syndrome, J. Am. Soc. Nephrol. 25 (4) (2014) 687–692.